Rigid-Rod Complex of a Cationic Poly(*p*-phenylene) and a Fluorinated Amphiphile

Andreas F. Thünemann,*,† Dirk Ruppelt,† Heimo Schnablegger,† and Jürgen Blaul‡

Max Planck Institute of Colloids and Interfaces, Am Mühlenberg, 14476 Golm, Germany, and Universität Karlsruhe, Polymer Institut, Kaiserstr. 12, 76128 Karlsruhe, Germany

Received November 23, 1999; Revised Manuscript Received January 24, 2000

ABSTRACT: The complexation of a cationic poly(*p*-phenylene) with tetraethylammonium perfluoro-1-octanesulfonate results in a highly fluorescent polymeric complex which forms cylindrical aggregates in solution and a columnar mesomorphous structure in the solid state. Two columns per unit cell are arranged in a rectangular two-dimensional lattice with lattice constants of 5.2 and 3.3 nm. A remarkably large phase width which varies from −50 to 300 °C, as determined by small-angle X-ray scattering and differential calorimetry, was found. The optical properties of the complex in solution and in the solid state were investigated using UV−vis and fluorescence spectroscopy.

Introduction

Substituted rigid-rod-like polymers with conjugated backbones are attractive building blocks for photonic devices. They facilitate the control of microscopic order as well as a predictable and defined molecular alignment.[1] Typical representatives of this class of molecules are poly- and oligo(*p*-phenylene) which have been found to be efficient in the production of blue laser dyes.[2] Blue photoluminescence with a quantum yield of 30% in the solid state is the reason for using *p*-phenylenes in organic light-emitting diodes.[3−6] There have been numerous studies dedicated to trying to understand the electronic properties of these highly luminescent materials.[7,8] Theoretical and experimental findings on short-chain model compounds in the solid state show that the planarity of *p*-phenylenes, and therefore the optical properties, are affected by hydrostatic pressure and temperature.[9] The orientation and diffusion dynamics as well as the aggregation behavior of poly(*p*-phenylene)s and their dependence on concentrations and the amount of added salt have been investigated in detail by Wegner et al.[10−12] Recently it was shown that ultrathin films made of poly(*p*-phenylene)s show a complicated dependence on the underlying substrate, the degree of polymerization, and the preparation conditions.[13] Further, negatively charged poly(*p*-phenylene)s with hydrophobic moieties show a complex association behavior in solution which depends on the hydrophobic hydrophilic balance.[14] The structures obtained were considered to describe the behavior of biogenic materials with respect to the formation of well-defined superstructures.

The mesomorphous structures and the optical properties of a complex formed by a cationic poly(*p*-phenylene) with an anionic fluorinated amphiphile is the objective of the present paper. We report on the structure of the complex in solution and in the solid state by using a combination of wide- and small-angle X-ray scattering techniques, differential calorimetry, UV−vis, and fluorescence spectroscopy.

Experimental Section

Materials and Preparation. The synthesis of the cationic poly(*p*-phenylene) polyelectrolyte has been described elsewhere.[15,16] The number-average degree of the polymerization $P_n = 11$ was determined for the uncharged polymer by vapor osmometry. A polydispersity of $M_w/M_n \approx 2$ is characteristic for polymers prepared by Pd-catalyzed polycondensation.[17,18] The polyelectrolyte was purified by serum replacement with ultrapure water (Milli-Q plus) in a stirred cell (Amicon) equipped with a regenerated cellulose filtration membrane (Millipore; pore size 30 000 nominal molecular weight limit). Afterward the retentate was freeze-dried.

Perfluoro-1-octanesulfonic acid, tetraethylammonium salt (98%, Aldrich), and methanol (HPLC grade, Aldrich) was used as delivered.

For complexation 220 mg (6.4 mmol of cationic groups) of the cationic poly(*p*-phenylene) and 400 mg (6.4 mmol) of perfluoro-1-octanesulfonic acid, tetraethylammonium salt, were dissolved, each in 20 mL of water (Millipore). Both solutions were heated to 80 °C and treated with ultrasound for 10 min. Then the polymer solution was added slowly to the surfactant solution. The complex was obtained as a brownish precipitate and separated. The solid was washed five times with 20 mL of hot water (60 °C) and dried for 12 h at reduced pressure (0.1 mbar).

Measurements. Wide-angle X-ray scattering (WAXS) measurements were carried out with a Nonius PDS120 powder diffractometer in transmission geometry. A FR590 generator was used as the source of Cu Kα radiation. Monochromatization of the primary beam was achieved by means of a curved Ge crystal, and the scattered radiation was measured with a Nonius CPS120 position-sensitive detector with a resolution in 2θ of 0.018°. We performed the small-angle X-ray scattering experiments of complex solutions with a Kratky compact camera (Anton Paar, Austria), equipped with a stepping motor and a counting tube with an impulse-height discriminator. The light source was a conventional X-ray tube with a fixed copper target operating at 40 mA and 30 kV. No monochromator (except the built-in impulse-height discriminator of the detector) was used. Instead, the Kβ contributions were numerically accounted for in the subsequent desmearing procedure which is included in the program ITP[19−21] which transforms the scattering data into real space and gives radial pair distance distribution functions (PDDF). This program uses the equation

$$I(s) \propto \int_{r=0}^{\infty} p(r) \frac{\sin(2\pi rs)}{2\pi rs} \, dr \qquad (1)$$

† Max Planck Institute of Colloids and Interfaces.
‡ Universität Karlsruhe.

10.1021/ma991972y CCC: $19.00
Published on Web 03/03/2000

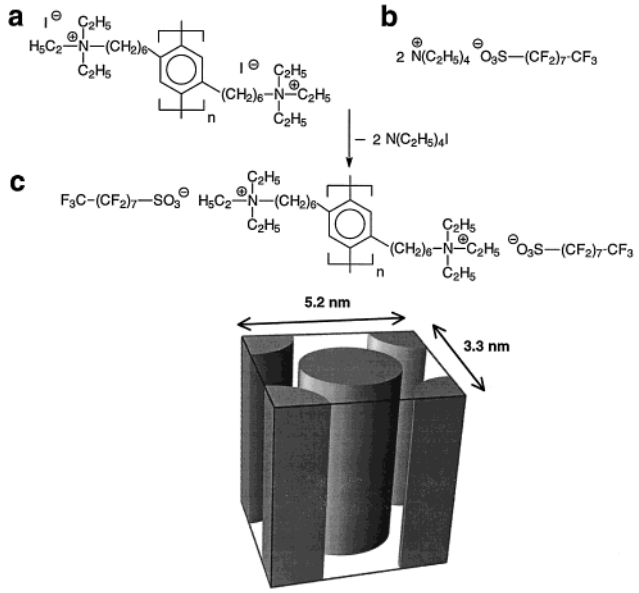

Figure 1. Sketch of the complex formation: (**a**) cationic poly(*p*-phenylene) as iodide; (**b**) perfluoro-1-octanesulfonic acid tetraethylammonium salt; (**c**) stoichiometric complex. The degree of polymerization is $P_n = 11$. The lower sketch shows a model of the proposed complex structure which contains two columns per unit cell ordered in a centered two-dimensional unit cell. The columns are formed by strands of poly(*p*-phenylene) molecules which were embedded in an amorphous matrix of fluorinated alkyl chains (not drawn).

where $p(r)$ is the radial PDDF to be calculated and $I(s)$ the desmeared scattering intensity expressed as a function of s. The scattering vector is defined in terms of the scattering angle θ and the wavelength λ of the radiation (Cu Kα = 0.154 nm). The length of the scattering vector is defined as $s = 2/\lambda \sin \theta$. The actual experimental data $J(s)$ can be expressed in terms of the desmeared intensity $I(s)$ (see eq 7 in ref 20), and both functions, $p(r)$ and $I(s)$, were computed in one step using the experimental scattering function $I(s)$, the wavelength-distribution data, and the corresponding beam profile of the experimental equipment. The temperature of the sample was adjusted to 25 ± 1 °C using a K-HR temperature controller (Anton Paar, Austria). The small-angle X-ray scattering measurements on solid samples were recorded with an X-ray vacuum camera with pinhole collimation (Anton Paar, Austria; model A-8054) equipped with image plates (type BAS III, Fuji, Japan). The image plates were read by a MACScience Dip-Scanner IPR-420 and IP reader DIPR-420 (Japan). Differential scanning calorimetry (DSC) measurements were performed on a Netzsch DSC 200 (Germany). The samples were examined at a scanning rate of 10 K/min by applying one cooling and two heating scans. UV−vis spectra were recorded on a UVICON spectrophotometer 931 (Kontron Instruments). The luminescence of films of the complex (400−600 nm thickness) was analyzed using a Perkin-Elmer LS-50B luminescence spectrometer with a front surface accessory. Excitation spectra were collected within the range of 200−320 nm. The emission wavelength was 340 nm, and the slits were 15/5 mm. Emission spectra were collected in the range of 300−500 nm. The excitation wavelength was 280 nm, and the slits were 15/5 mm.

Results and Discussion

The complexation of the cationic poly(*p*-phenylene) **a** with perfluoro-1-octanesulfonate **b** was performed from aqueous solution, resulting in the polymeric complex **c** which was obtained as a yellow-brownish precipitate. A schematic view is given in Figure 1.

Structure in Solution. The structure of the complex in methanol solution was investigated by small-angle X-ray scattering. Concentrations of 0.2−2% (w/w) were used. The shape of the scattering curves did not change significantly within the concentrations investigated. From this we concluded that the scattering entities in the solution, which can tentatively be assigned to cylindrical aggregates of molecules of the complex, did not change significantly. The absence of minima in the scattering curve indicates a relatively high polydispersity of these aggregates. For these experiments, scattering data were obtained with a Kratky camera using a slit collimation. The data were therefore desmeared.[19−21] Smeared and desmeared scattering curves are shown in Figure 2. The curves obey Porod's law at values of the scattering vector higher than 0.2 nm^{-1}.

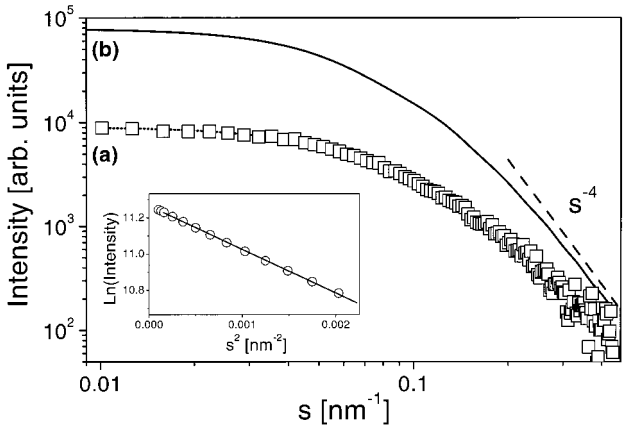

Figure 2. Small-angle X-ray scattering curves obtained for a dilute solution (1% (w/w)) of **c** in methanol. (a) The data points as measured with a Kratky camera (squares) and the smoothed data points (dotted line). (b) Desmeared scattering curve as calculated from (a) taking into account the geometry of the beam and the wavelength distribution. The inset shows a Guinier plot of I from which a radius of gyration of 4.3 nm was determined.

Porod's law[22,23] is given by

$$l_p = \frac{2\pi \int_0^\infty sJ(s)\,\mathrm{d}s}{\lim_{s\to\infty} 4\pi^2 s^3 J(s)} \qquad (2)$$

for the measurement with a slit focus and

$$l_p = \frac{4\pi \int_0^\infty s^2 I(s)\,\mathrm{d}s}{\lim_{s\to\infty} 2\pi^3 s^4 I(s)} \qquad (3)$$

for the desmeared scattering curve or the measurement with a pinhole focus. J is the slit-smeared scattering intensity, I the desmeared intensity, and l_p the average cord length. Such a scaling law is a strong indication of a two-phase system with sharp interface boundaries, namely that between complex aggregates and the solvent. This finding seems to be surprising, but it is consistent with the high amount of fluorinated segments of the complex (58% (w/w)). The fluorinated segments form the cores of aggregates of the complex. They are highly incompatible with the nonfluorinated solvent. Furthermore, the scattering intensity is proportional to the square of the large electron density difference between fluorinated and nonfluorinated regions. Therefore, it seems likely that a steplike electron density transition between an aggregate and solvent is a realistic structural feature of the complex in solution. The values given by eqs 1 and 2 result in a consistent

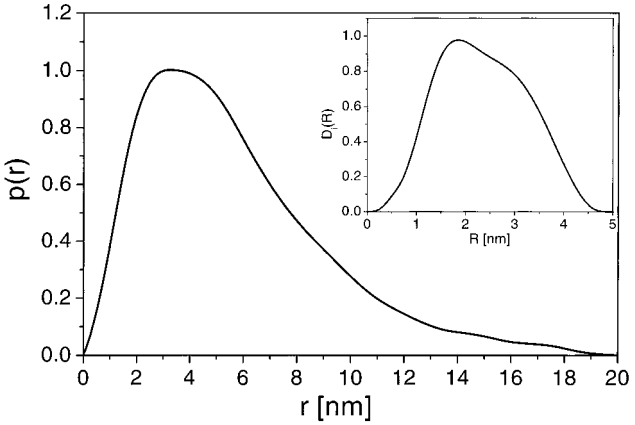

Figure 3. Distance distribution function calculated from the scattering curve. The inset shows the diameter distribution of the cylindrical complex aggregates calculated from the distance distribution function, assuming a constant length of 14 nm.

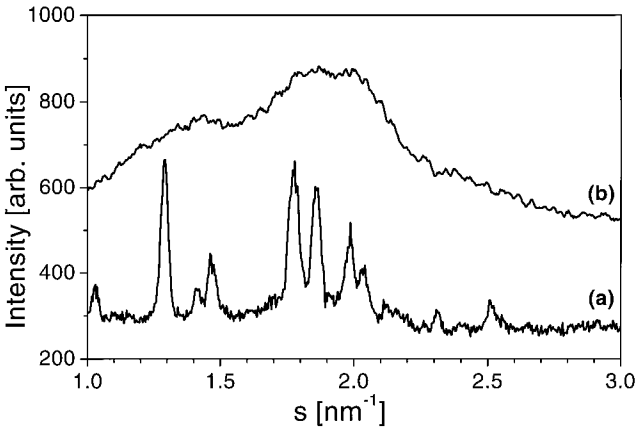

Figure 4. Wide-angle X-ray scattering of the perfluoro-1-octanesulfonic acid, tetraethylammonium salt (curve a), and of the complex (curve b).

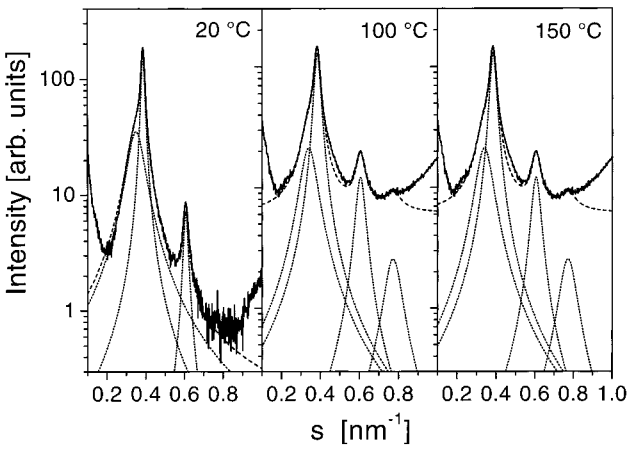

Figure 5. Small-angle X-ray scattering of the solid complex at different temperatures. The solid lines represent the scattering data, and the dashed lines are the curve fits, which are superpositions of Lorentzian peak profiles. For clarity of the position and width of the peak profiles, the individual peaks are given (dotted lines).

Table 1. Small-Angle X-ray Data of b[a]

	s_{obsd} [nm^{-1}]			
(hk)	T = 20 °C	T = 100 °C	T = 150 °C	s_{calcd} [nm^{-1}]
11	0.350	0.340	0.340	0.358
20	0.386	0.385	0.380	0.385
02	0.607	0.606	0.606	0.606
22		0.772	0.772	0.718

[a] Reflex positions and Miller indices are given for the two-dimensional ordered lattices at 20, 100, and 150 °C. The scattering vector is defined as $s = 2/\lambda \sin \theta$.

average cord lengths of 1.9 ± 0.1 nm. The connection between l_p, the radius R, and the height H for a cylindrical aggregate is given as $1/l_p = 1/(2R) + 1/(2H)$. Therefore, in the case of large cylinders l_p, is close to its diameter whereas in the other cases it is smaller. Here it can be assumed that l_p is slightly smaller than the diameter of the aggregates. The radius of gyration R_g of the aggregates was determined to be 4.3 ± 0.1 nm. This was obtained from a Guinier plot (see Figure 2, inset). From the gyration radius the height of a cylindrical particle can be calculated[24,25] by $R_g^2 = R^2/4 + H^2/12$. The height was calculated to be about 13−14 nm by approximating $R \approx l_p/2$. A further evaluation of the scattering data was achieved by the indirect Fourier transform method.[20,26] This method transforms the experimental scattering function into a pair distance distribution function (PDDF), which is shown in Figure 3. It can be seen from the PDDF that the maximum length of the complex aggregates is about 18 nm, and the predominant lengths of the aggregates are between 10 and 14 nm. From the second moment of the PDDF the radius of gyration was determined to be 4.7 nm. The cross-section distribution of the aggregates was determined using an optimized regularization program of Schnablegger and Glatter.[27] For stable numerical calculations of the polydispersity of the cylindrical cross sections the lengths of the cylinders were taken to be constant (14 nm). Obviously the lengths are polydisperse, but the best fitting average value was determined to be 14 nm. The result is shown in Figure 3 (inset). It can be seen there that the distribution is relatively broad, ranging from about 1 to 4 nm, as expected from the absence of minima in the scattering curve. The distribution has a maximum at 1.9 nm, which is identical to l_p, and an average value of 2.3 nm.

Structure in the Solid State. Complex films were prepared from complex solution in methanol by the common solvent casting procedure.[28] Their structure was investigated by wide- and small-angle X-ray scattering. A number of sharp reflections are found in the wide-angle diagram of **b**, which is a highly crystalline compound, while no sharp reflections are present in those of **a** and **c**. This proves that neither **a** nor **c** is a partially crystalline material (see Figure 4). The broad reflection centered at 2 nm^{-1} in the diagram of **c** is interpreted as resulting from the scattering of the fluorinated chains with a short-range order and with an average chain-to-chain distance of about 0.5 nm.[29] In recent years it has been found that a number of polyelectrolyte−surfactant complexes form highly ordered mesomorphous structures in the solid state.[30,31] Therefore, it was probable that **c** can be ordered on a length scale of several nanometers. This assumption was confirmed by small-angle X-ray scattering measurements of the solid sample. In Figure 5 it can be seen that a number of reflections are present in the small-angle diagrams at temperatures of 20, 100, and 150 °C and that the reflex positions that where determined by fitting Lorentzian profiles to the scattering curves are essentially identical. (Reflex positions are given in Table 1.) Obviously there should be a thermal expansion of the material when the temperature is raised to 150 °C.

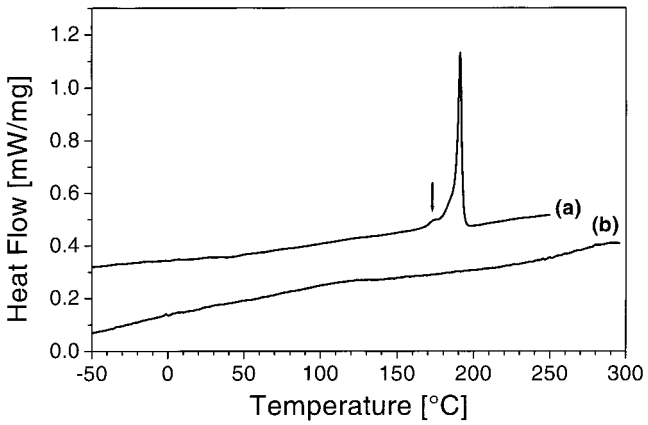

Figure 6. DSC traces of perfluoro-1-octanesulfonic acid, tetraethylammonium salt (curve a), and of the complex (curve b).

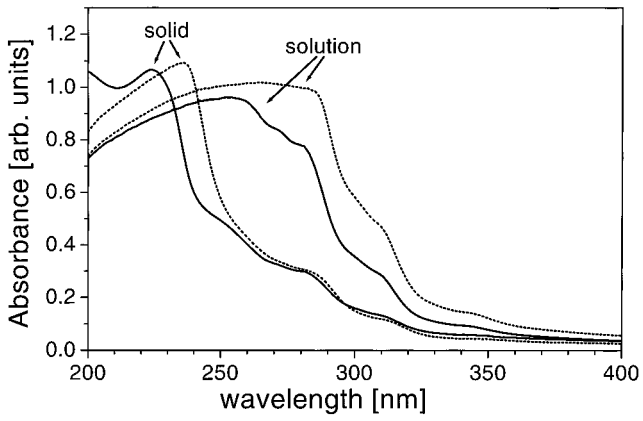

Figure 7. Absorption spectra of the cationic poly(*p*-phenylene) **a** (dotted lines) and of the complex **c** (solid lines). The concentrations of both solutions in methanol was 10^{-2}% (w/w).

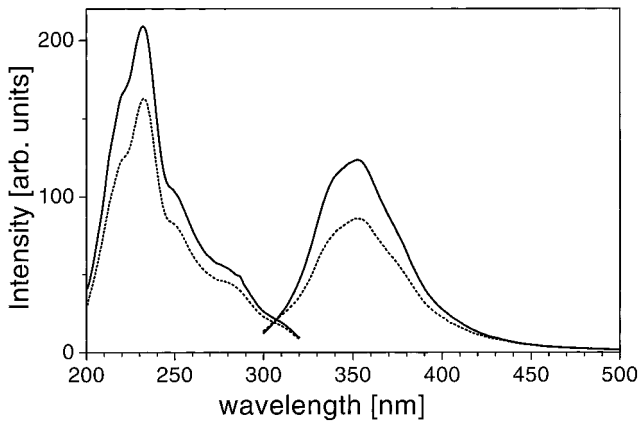

Figure 8. Fluorescence excitation and emission spectra of **a** (dashed lines) and of **c** (solid lines) in solution of 10^{-4}% (w/w with respect to the polymer) in methanol.

However, this effect changes the values of the cell lattice only about 1−2%. For example, the position of the most intense reflection corresponds to Bragg spacings of 2.59 nm (20 °C), 2.60 nm (100 °C), and 2.63 nm (150 °C). Only the background, due to thermal fluctuations, and the widths of the reflections increase with increasing temperature. The correlation lengths of the mesomorphous structures were found to decrease in the line 50 nm (20 °C), 35 nm (100 °C), 30 nm (150 °C) as was expected. A model that describes the scattering pattern sufficiently is the arrangement of flattened cylinders in a two-dimensional lattice (see Figure 1). The cell dimensions of the unit cells are 5.2 and 3.3 nm with two columns per unit cell. Each column contains three to four poly(*p*-phenylene) strands which are embedded in a matrix of fluorinated alkyl chains. Each strand is bound ionically to the matrix. The most probable orientation of the main axes of the poly(*p*-phenylene) molecules is perpendicular to the two-dimensional unit cell.

A tilted orientation of the complexed molecules cannot be excluded on the basis of the scattering data. For this 00*l* reflections have to occur. The absence of 00*l* reflections can be explained as a result of the polydispersity of **a** which prevents an arrangement of the strands of complexed molecules in a three-dimensional ordered superstructure. For complexes of monodisperse poly(*p*-phenylene) molecules we expect a three-dimensional order such as a smectic H structure. By differential calorimetry it was confirmed that the two-dimensional columnar structure is stable over a wide range of temperatures. It can be seen in Figure 6 (curve a) that two phase transitions are present for **b**: a weak endothermic transition at 173 °C and a strong one at 191 °C. The former is probably a solid/solid phase transition from one crystalline phase α to a second crystalline phase β. Then the latter is a melting transition of the β phase. By contrast, no transition was found in the range of −50 to 300 °C for **c**. The first and the second heating traces are identical. Together with the results from the small-angle scattering, we conclude that the supramolecular structure of the complex is stable within this remarkably large range of temperatures.

Optical Properties. The absorption spectra of diluted solutions of **a** and **c** in methanol and of thin solid films are displayed in Figure 7. It can be seen that the spectra of **a** and **c** are similar, but compared to those of **a**, the spectra of **c** show hypsochromic shifts of about 10 nm. An absorption maximum at 265 nm and two shoulders at 309 and 340 nm were found for the solution of **a** while, for the solid sample, the maximum was shifted to the shorter wavelength at 237 nm; shoulders appeared at 285 and 310 nm. This is indicative of a further reduction of the conjugation of the polymeric backbone in the solid state compared to the conjugation length in solution, which is known to be low in oligo-*p*-phenylenes.[9] The same tendency was observed for the complex. Here, an absorption maximum at 255 nm and three shoulders at 280, 309, and 340 nm were found for the solution. For the film the maximum was shifted to a shorter wavelength at 224 nm, and the shoulders appeared at 250, 280, and 308 nm. Figure 8 shows the fluorescence excitation and emission spectra of **a** (dotted lines) and **c** (solid lines) in solution. The excitation wavelength was 280 nm and the emission wavelength 340 nm. It can be seen that the excitation spectra of **a** and **c** are essentially identical. Bands at 223, 243, 257, and 283 nm are observed for **a** and at 223, 243, 257, and 280 nm for **c**, but the intensity of **c** is higher than that of **a**. The emission maxima of **a** and **c** are found at 353 nm. But the intensity of the latter is higher. Additionally, the fluorescence measurements were performed on thin films of **a** and **c** (see Figure 9, film thicknesses were about 200−600 nm). Again it was found that the shapes of the spectra of **a** and **b** are similar. The excitation maxima of **a** and **c** are at 221, 232, 250, and 283 nm, and the emission maxima are at 339 nm (**a**) and 346 nm (**c**). As in solution it was

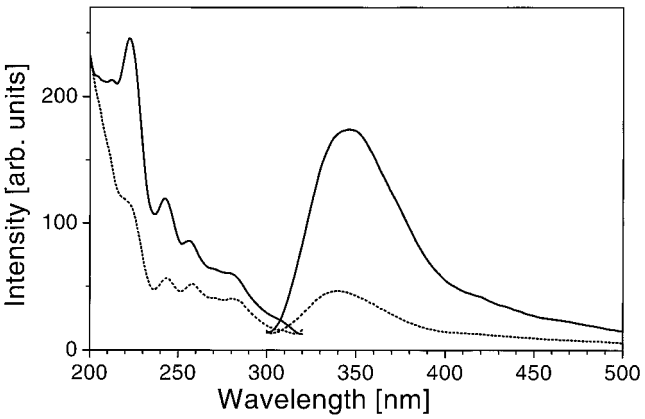

Figure 9. Fluorescence excitation and emission spectra from films of **a** (dashed lines) and of **c** (solid lines). The film thickness was about 200 nm.

observed that the fluorescence intensities of **c** are significantly higher that those of **a**. Tentatively, we interpret the higher fluorescence intensity of the complex as being due to the influence of the fluorinated side chains. They lower the refractive index, and they separate the polymer chains. This reduces the probability of a radiationless decay of excited states, and it therefore enhances the external quantum efficiency of the polymeric chromophore. It was reported recently that a better separation of the polymer chains of an electroluminescent polymer reduces the nonradiative decay of excitons.[32] On the basis of these preliminary results, it can be assumed that the complexation of highly fluorescent polymers may result in enhanced properties of diodes of polymeric complexes,[33] for example, a higher external quantum efficiency.

Conclusions

A new mesomorphous columnar complex with interesting fluorescent properties was prepared from a rigid-rod-like polyelectrolyte and a fluorinated surfactant. Two columns per unit cell are arranged in a two-dimensional lattice with lattice constants of 5.2 and 3.3 nm. Within these cells the fluorinated chains represent an amorphous matrix in which the rigid-rod-like polymer molecules are embedded. Matrix and polymer are linked via ionic bonds. The phase width of this new highly ordered material is remarkably large: it ranges from −50 to 300 °C. The combination of the high order and the high stability with its easy processability for film formation makes this highly fluorinated complex interesting for optoelectronic applications such as polymeric LED's.

Acknowledgment. The authors thank Prof. Dr. Ballauff for helpful remarks and Dr. C. Burger for calculating the ray-traced sketch of the unit cell in Figure 1. The financial support by the Max Planck Society is gratefully acknowledged.

References and Notes

(1) Neher, D. *Adv. Mater.* **1995**, *7*, 691.
(2) Furumoto, H. W.; Ceccon, H. L. *J. Quantum Electron.* **1970**, *6*, 262.
(3) Hosokawa, C.; Higashi, H.; Kusumoto, T. *Appl. Phys. Lett.* **1993**, *62*, 3238.
(4) Graupner, W.; Grem, G.; Meghdadi, F.; Paar, Ch.; Leising, G.; Scherf, U.; Müllen, K.; Fischer, W.; Stelzer, F. *Mol. Cryst. Liq. Cryst.* **1994**, *256*, 549.
(5) Leising, G.; Tasch, S.; Graupner, W. In *Handbook of Conducting Polymers*, 2nd ed.; Marcel Decker: New York, 1997; p 847.
(6) Cimrova, V.; Schmidt, W.; Rulkens, R.; Schulze, M.; Meyer, W.; Neher, D. *Adv. Mater.* **1996**, *8*, 585.
(7) Piaggi, A.; Lanzani, G.; Bongiovanni, G.; Mura, A.; Graupner, W.; Meghdadi, F.; Leising, G. *Phys. Rev. B* **1997**, *56*, 10133.
(8) Graupner, W.; Meghdadi, F.; Leising, G.; Lanzani, G.; Nisoli, M.; De Silvestri, S.; Fischer, W.; Stelzer, F. *Phys. Rev. B* **1997**, *56*, 10128 and references therein.
(9) Guha, S.; Graupner, W.; Resel, R.; Chandrasekhar, M.; Chandrasekhar, H. R.; Glaser, R.; Leising, G. *Phys. Rev. Lett.* **1999**, *82*, 3625.
(10) Liu, T.; Rulkens, R.; Wegner, G.; Chu, B. *Macromolecules* **1998**, *31*, 6119.
(11) Petekidis, G.; Vlassopoulos, D.; Fytas, G.; Rülkens, R.; Wegner, G. *Macromolecules* **1998**, *31*, 6129.
(12) Petekidis, G.; Vlassopoulos, D.; Fytas, G.; Rülkens, R.; Wegner, G.; Fleischer, G. *Macromolecules* **1998**, *31*, 6139.
(13) Brunner, S.; Caseri, W. R.; Suter, U. W.; Hähner, G.; Brovelli, D.; Spencer, N. D.; Vinckier, A.; Rau, I. U.; Galda, P.; Rehan, M. *Langmuir* **1999**, *15*, 6333.
(14) Rulkens, R.; Wegner, G.; Thurn-Albrecht, T. *Langmuir* **1999**, *15*, 4022.
(15) Rau, I. U.; Rehahn, M. *Acta Polym.* **1994**, *45*, 3.
(16) Brodowski, G.; Horvath, A.; Ballauff, M.; Rehahn, M. *Macromolecules* **1996**, *29*, 6962.
(17) Schmitz, L.; Ballauf, M. *Polymer* **1995**, *36*, 879.
(18) Galda, P. Dissertation, Karlsruhe, 1994.
(19) Glatter, O. *Acta Phys. Austriaca* **1977**, *47*, 83.
(20) Glatter, O. *J. Appl. Crystallogr.* **1977**, *10*, 415.
(21) Glatter, O. *J. Appl. Crystallogr.* **1979**, *12*, 166.
(22) Porod, G. *Kolloid-Z.* **1951**, *124*, 83.
(23) Porod, G. *Kolloid-Z.* **1952**, *125*, 51.
(24) Mittelbach, P. *Acta Phys. Austriaca* **1964**, *19*, 53.
(25) Watson, A. J. C.; Primo, E. *International Tables of Crystallography;* 1999; Vol. C, Chapter 2.6.
(26) Glatter, O. *J. Appl. Crystallogr.* **1980**, *13*, 577.
(27) Schnablegger, H.; Glatter, O. *J. Colloid Interface Sci.* **1993**, *158*, 228.
(28) Antonietti, A.; Conrad, J.; Thünemann, A. *Macromolecules* **1994**, *27*, 6007.
(29) Thünemann, A. F.; Lochhaas, K.-H. *Langmuir* **1998**, *14*, 4898.
(30) Ober, C.; Wegner, G. *Adv. Mater.* **1997**, *9*, 17.
(31) Antonietti, M.; Burger, C.; Thünemann, A. *TRIP* **1997**, *5*, 262.
(32) Jang, M. S.; Song, S. Y.; Lee, J. I.; Shim, H. K.; Zyung, T. *Macromol. Chem. Phys.* **1999**, *200*, 1101.
(33) Thünemann, A. F. *Adv. Mater.* **1999**, *11*, 127.

MA991972Y